Small-Angle Neutron Scattering Studies on Sodium Dodecylbenzenesulfonate–Tetra-*n*-butylammonium Bromide Systems

Sanjeev Kumar, Daksha Sharma, Deepti Sharma, and Kabir-ud-Din*

Department of Chemistry, Aligarh Muslim University, Aligarh 202 002, India

ABSTRACT: A phase study was completed on aqueous sodium dodecylbenzenesulfonate (SDBS) and tetra-*n*-butylammonium bromide (Bu_4NBr) systems, and consolute boundaries were drawn through cloud points. Samples were selected from both miscibility regions [under the lower consolute boundary (LCB) and above the upper consolute boundary (UCB)] for small-angle neutron scattering (SANS) studies. In the first set of experiments, the effect of varying Bu_4NBr concentration on micellar parameters of 100 mM SDBS was studied at 30°C. The pure SDBS micelle has an aggregation number (n_s) of 51, and the effective charge on the monomer (α) is 0.17. With the addition of Bu_4NBr, the n_s of SDBS micelles increases while α decreases. The system with [Bu_4NBr] = 39.5 mM (an above-UCB sample) showed clouding near room temperature (≈29°C) and had a high n_s value (300) and a low α (= 0.09). The data indicated that the micelles lose ionic character in the presence of Bu_4NBr. The temperature effect on this sample shows that α remains almost constant, while n_s decreases on heating. A similar effect was observed with samples of lower Bu_4NBr concentration (32 or 25 mM) in the presence of 100 mM SDBS. The same type of temperature effect was seen on a sample of under-LCB region (50 mM SDBS + 32 mM Bu_4NBr); the n_s values increased significantly as the LCB was approached. The overall SANS observations suggest that the micelles have low ionic character together with high n_s values (a case of micellar growth) near LCB/UCB.

Paper no. S1505 in *JSD 9*, 77–82 (Qtr. 1, 2006).

KEY WORDS: Cloud point, consolute boundaries, small-angle neutron scattering, sodium dodecylbenzenesulfonate, tetra-*n*-butylammonium bromide.

The observation of partial miscibility in binary surfactant/water micellar solutions is commonplace (1–5). Reports of both lower and upper consolute curves for nonionic and zwitterionic surfactants are frequent (1,2). There even exist a few reports of lower consolute curves for ionic surfactants in water (3,6–8).

The phase boundary curve of the miscibility gap is commonly known as the "cloud" or "consolute" curve (9) in view of the pronounced turbidity of the solutions close to the phase separation. Initially this clouding was ascribed to an increase in size and aggregation number, n_s (10), of the micelles and to the formation of giant micelles, which were believed eventually to become insoluble in water (11). Later, it was realized that the clouding results from the clustering of micelles as a result of attractive intermicellar interactions, and the term "coacervate curve" was coined for concentrated micellar solutions with a conjectured liquid-like packing of the micelles (12,13). In the last two decades considerable attention has been paid to scattering behavior (14–17) close to the critical point of these solutions. Hayter *et al.* (15) concluded from small-angle neutron scattering (SANS) experiments that the observed increase in the forward scattering is due to the formation of larger particles consisting of spherical micelles of fixed size. Strey and Pakusch (18) suggested that the region of the isotropic solution [below the lower consolute boundary (LCB)] may be divided into three sections: a region of single spherical micelles at low surfactant concentrations and low temperatures, aggregates of micelles in an intermediate range at higher mass fractions of the surfactant and higher temperatures, and a critical region that is dominated by critical point fluctuations. This picture is widely accepted for the below-LCB region although presently there is little knowledge about structures near the LCB. Kumar *et al.* (17) concluded that micellar growth takes place as the system approaches the cloud point (CP) (17).

Recently interest has focused on the possibility that upper or lower critical points could occur within clear regions above or below the consolute boundaries (14,19–21). An upper consolute loop within a lamellar phase has been reported for binary anionic and cationic surfactants in water. However, lower and upper consolute loops are much rarer in the same system. Here, sections of lower and upper consolute boundaries have been produced in experiments in which the temperature was varied and the effect on the visual appearance of solutions (prepared in H_2O) was determined. For this purpose, sodium dodecylbenzenesulfonate (SDBS) was used as the surfactant and tetra-*n*-butylammonium bromide (Bu_4NBr) as the salt. SANS studies

*To whom correspondence should be addressed.
E-mail: kabir7@rediffmail.com

Abbreviations: BARC, Bhabha Atomic Research Centre; Bu_4NBr, tetra-n-butylammonium bromide; CP, cloud point; LCB, lower consolute boundary; n_s, aggregation number; SANS, small-angle neutron scattering; SDBS, sodium dodecylbenzenesulfonate; SDS, sodium dodecyl sulfate; UCB, upper consolute boundary.

were performed in the clear region above the UCB and below the LCB. For the SANS measurements, samples were prepared in D_2O (no phase study was conducted with D_2O). SANS data from 100 mM sodium dodecylsulfate (SDS) were also collected for comparison purposes.

EXPERIMENTAL PROCEDURES

SDBS (≥99%; TCI, Japan), SDS (>99%, Fluka, St. Gallen, Switzerland), and Bu_4NBr (≥99%; Fluka) were used as received. Solvent D_2O of 99.4% purity was supplied by the Heavy Water Division, Bhabha Atomic Research Centre (BARC;, Mumbai, India). Deionized double-distilled water was used for phase studies (CP-measurements). The CP values for the sample solutions containing different fixed concentrations of SDBS and Bu_4NBr were obtained by the method reported elsewhere (6–8). The measurements were performed on a SANS spectrometer having an accessible wave-vector transfer, Q (= $4\pi\sin\theta/\lambda$, where 2θ and λ are the scattering angle and mean wavelength of incident neutrons, respectively), range between 0.018 and 0.32 $Å^{-1}$. The experiments used $\lambda = 5.2$ Å with a sample-to-detector distance of 1.8 m. The angular distribution of the scattered neutrons was recorded with a one-dimensional position-sensitive detector.

The raw data were corrected for background, empty cell scattering, and sample transmission. The corrected intensities were normalized to absolute cross-section units and thus $d\Sigma/d\Omega$ vs. Q was obtained (22). The experimental data points were fitted by adopting the routines described by Hayter and Penfold (23) and Chen and coworkers (24,25). The data have not been corrected for resolution effects. Analysis of a limited set of data showed that resolution corrections do not alter the n_s of the micelle. The residuals in the fitting were negligible.

The relevant SANS theory is summarized as follows: For homogeneous monodisperse micelles of volume V_P present at a number density n_P and of coherent scattering length density ρ_P, dispersed in a medium of scattering length density ρ_m, the coherent differential scattering cross-section ($d\Sigma/d\Omega$) is written as (23,26,27)

$$d\Sigma/d\Omega = n_P V^2_P (\rho_P - \rho_m)^2 \cdot P(Q) \cdot S(Q) + B \qquad [1]$$

where $P(Q)$ is the single (orientationally averaged) particle form factor, which depends on the size and shape of the particle, and $S(Q)$ is the interparticle structure factor. B is a constant term that represents incoherent scattering, which is mainly due to hydrogen atoms in the sample.

For analysis, the micelles were assumed to be monodisperse, prolate ellipsoids ($a = b \neq c$), where the sphere is a special case. It may be mentioned, however, that elongated micelles usually tend to be of varying size and may not be monodispersed, but Equation 1 is not valid for polydispersed systems. It was further assumed that the micelles have a hydrophobic core composed of dodecyl chains and a hydrated hydrophilic shell composed of head groups ($-SO_3^-$), a fraction of Na^+, Bu_4N^+, and solvent molecules (D_2O). The position and interactions of Bu_4N^+ near the anionic micellar surface are detailed elsewhere (6–8). Although there are limitations of such assumptions, it is not possible to get information on size distribution of micelles from the present data because of the involvement of too many unknown parameters in the data analysis. Thus, in the present analysis, the system is assumed to be monodisperse to avoid additional complexities.

The n_s for the micelle is related to V_P by the relation $n = V_P/v$, where v is the volume of surfactant monomer. $P(Q)$ for anisotropic micelles (e.g., ellipsoidal) is given by

$$P(Q) = \int [F(Q, \mu)]^2 \, d\mu \qquad [2]$$

The form factor $F(Q, \mu)$ is given by

$$F(Q, \mu) = 3(\sin\omega - \omega\cos\omega)/\omega^3 \qquad [3]$$

where $\omega = Q[a^2\mu^2 + c^2(1 - \mu^2)]^{1/2}$ and μ is the cosine of the angle between the axis of revolution and Q. Therefore, $P(Q)$ is dependent on both the semiminor (a) and semimajor (c) axes.

The volume of SDBS monomer was taken to be 498 $Å^3$, as given by Tanford's formula (28). $S(Q)$ was calculated using standard methods (27). This theory is applicable if there is no angular correlation between the micelles, which is reasonable for charged micelles. It may be mentioned that a satisfactory data analysis method for charged rod-shaped micelles has not yet been developed. In this analysis, the calculated spectra have three parameters, viz., the effective charge per monomer (α), a, and c or n_s.

The SANS data were analyzed using the method discussed above and parameters α, a, c, and n_s were computed. Solid lines in $d\Sigma/d\Omega$ vs. Q curves are the calculated fits.

RESULTS AND DISCUSSION

The temperature /Bu_4Nbr concentration phase diagrams (Figs. 1, 2) show that the nature of the appearance of consolute boundaries is dependent on SDBS concentration. With 50 mM SDBS, only LCB was realized whereas with 100 mM SDBS both LCB and UCB were realized by increasing the temperature and Bu_4NBr concentration. As mentioned earlier, the SANS data were obtained with samples prepared in D_2O. However, no phase study was performed in D_2O, and it is believed that the samples chosen for SANS measurements belong to the clear regions above the UCB and under the LCB.

Several SANS spectra were obtained with SDBS solutions and compared with a 100 mM SDS solution (Fig. 3) before the actual experiments were performed. Inspection of Table 1 suggests that micelles are bigger in the case of SDS than SDBS. Comparison of SDS and SDBS molecules shows that SDBS molecule should be longer than SDS owing to

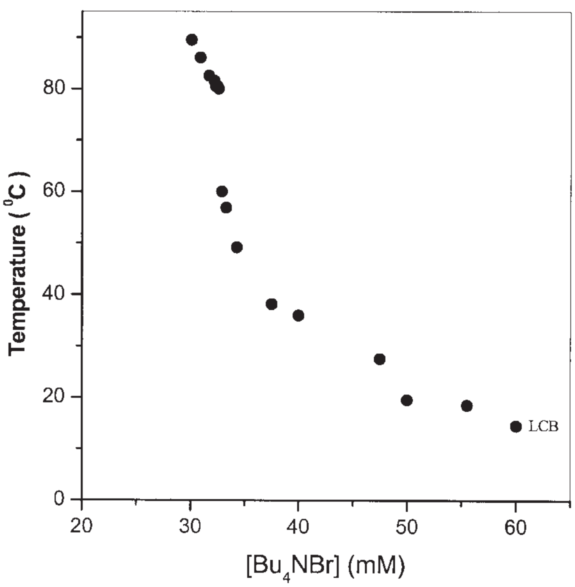

FIG. 1. Temperature vs. Bu_4NBr phase diagram for the 50 mM SDBS/Bu_4NBr/H_2O system. The curve represents the lower consolute boundary (LCB). Bu_4NBr, tetra-*n*-butylammonium bromide; SDBS, sodium dodecylbenzenesulfonate.

the presence of a benzene ring in the former (Scheme 1). But $d\Sigma/d\Omega$ is higher in the case of SDS (Fig. 3). The drop in n_s due to the ring may result from the presence of a voluminous group in the head group region. As a result, the head groups cannot come closer than a certain limit due to repulsive interactions of the π-electron cloud of the benzene rings present in the monomers of the micelles. To alleviate these unfavorable electrostatic consequences, the hydrocarbon chains in the micelles of SDBS take on folded conformations, and hence SDBS micelles would experience a relatively wetter environment than the SDS ones. In comparison, the hydrocarbon chains could be more extended in case of SDS, and the terminal CH_3 group is buried deep inside the micellar core. Hence *a* of SDS is expected to be more than that of SDBS. The higher values of n_s and *a* for SDS confirm these propositions (Table 1).

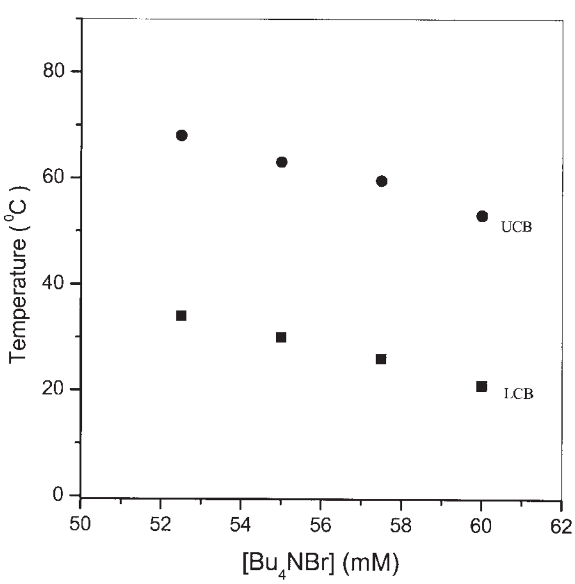

FIG. 2. Temperature vs. Bu_4NBr concentration phase diagram for the 100 mM SDBS/Bu_4NBr/H_2O system. The two sections of curves belong to the LCB (■) and the upper consolute boundary (UCB, ●). For abbreviations see Figure 1.

TABLE 1
Micellar Parameters for x mM Surfactant Obtained from Hayter–Penfold-Type Analysis[a] at 30°C

x (mM)	n_s	α	c (Å)	a = b (Å)	c/a
100 (SDS)	72	0.24	25.9	15.2	1.70
100 (SDBS)	51	0.17	34.1	13.3	2.56
50 (SDBS)	44	0.18	30.6	13.1	2.33

[a]SDS, sodium dodecyl sulfate; SDBS, sodium dodecylbenzenesulfonate; ns, aggregation number; α, effective charge of the monomer; a–c, ellipsoid dimensions.

SANS spectra of 100 mM SDBS with added Bu_4NBr are presented in Figure 4. Each spectrum contains a well-defined interaction peak, characteristic of dispersions of charged particles, which seems just to disappear at 39.5 mM Bu_4NBr. This change occurs because of micellar growth and screening of the repulsive forces between the particles. The micellar growth is consistent with the viscosity and SANS results obtained for the same salt added to aqueous SDS (29,30). The higher n_s and low α values are also consistent with micellar growth in these systems with the addition of Bu_4NBr (Table 2).

On the basis of the studies just described, the system 100 mM SDBS + 39.5 mM Bu_4NBr, which is expected to belong to the clear region above the UCB (as phase studies in D_2O samples were not performed), was chosen. The system showed CP ~ 29°C. The SANS spectra of this system at different temperatures are given in Figure 5. At 30°C, $d\Sigma/d\Omega$-diverges in the region of low *Q* (<0.02 $Å^{-1}$). This type of behavior usually occurs with ionic micelles at higher salt concentrations (31) or with nonionic micelles at higher temperatures (32). With a higher value of n_s and low α (Table 3), it can be safely assumed that the micelles in this system have some characteristics of nonionic surfactant systems. Interestingly, at higher temperature (Fig. 5) there is a decrease in $d\Sigma/d\Omega$ in the low *Q* region, and at 80°C, an interaction peak starts reappearing. However, $d\Sigma/d\Omega$ remains independent of temperature in the region of large *Q* (>0.10 $Å^{-1}$). To further substantiate the temperature effect, SANS spectra were collected for lower concentrations of added Bu_4NBr (32 and 25 mM, Figs. 6 and 7, respectively). Lowering of $d\Sigma/d\Omega$ also occurred in these cases, with well-defined interaction peaks from which we can infer that the micelle

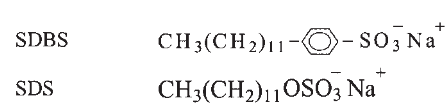

SCHEME 1

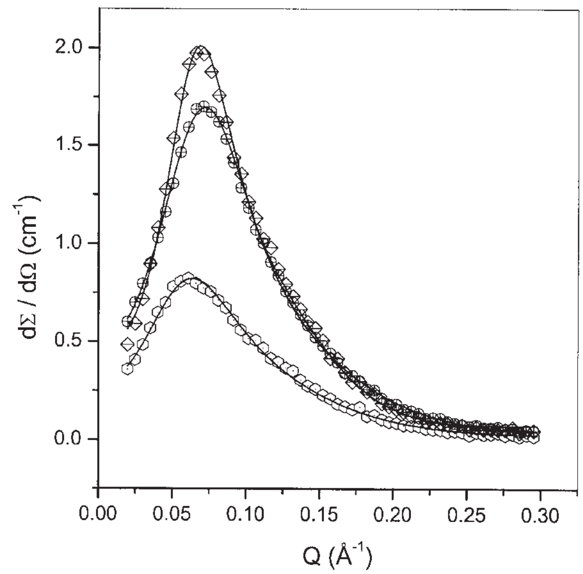

FIG. 3. Small-angle neutron scattering (SANS) spectra from different surfactant (SDS and SDBS) solutions at 30°C: (open hexagon with centered dot), 50 mM SDBS; (circle with cross), 100 mM SDBS; (diamond with horizontal line), 100 mM SDS. Solid lines are theoretical fits based on Hayter–Penfold-type analysis. SDS, sodium dodecyl sulfate; $d\Sigma/d\Omega$, coherent differential scattering cross-section; for other abbreviation see Figure 1.

characteristics are changed from nonionic to ionic with the rise of temperature. This is also supported by the increased α values obtained at higher temperatures (Table 5). However, this behavior is opposite to the behavior reported for

TABLE 2
Micellar Parameters for 100 mM SDBS + *x* mM Bu_4NBr Obtained from Hayter–Penfold-Type Analysis[a] at 30°C

x (mM)	n_s	α	*c* (Å)	*a* = *b* (Å)	*c*/*a*
0	51	0.17	34.1	13.3	2.56
5	58	0.17	37.8	13.7	2.76
15	105	0.10	62.2	14.7	4.23
25	192	0.10	109.2	15.4	7.09
32	228	0.09	126.8	15.9	7.97
39.5	300	0.09	162.6	16.4	9.91

[a]Bu_4NBr, tetra-*n*-butylammonium bromide; for other abbreviations see Table 1.

SDS + Bu_4NBr system where $d\Sigma/d\Omega$ increases with the increase in temperature (17). This may be due to the system's position in the phase diagram. The earlier reported system (17) seemingly is under the LCB while the present ones are above the UCB. This also shows that the position of a particular system in the phase diagram is important for the overall behavior.

The temperature effect on a system that is expected to be in the region under the LCB (50 mM SDBS + 32 mM Bu_4NBr; Fig. 8) is in sharp contrast with that observed with the systems above the UCB. Here, the temperature increase causes an increase in $d\Sigma/d\Omega$ at low Q whereas $d\Sigma/d\Omega$ is independent of the temperature in the large Q (>0.075 $Å^{-1}$) region. The increase in $d\Sigma/d\Omega$ with temperature rise at lower Q is, in a sense, similar to that observed in nonionic micellar solutions where interactions are dominated by van der Waals forces (32). Here, no interaction peak is observed

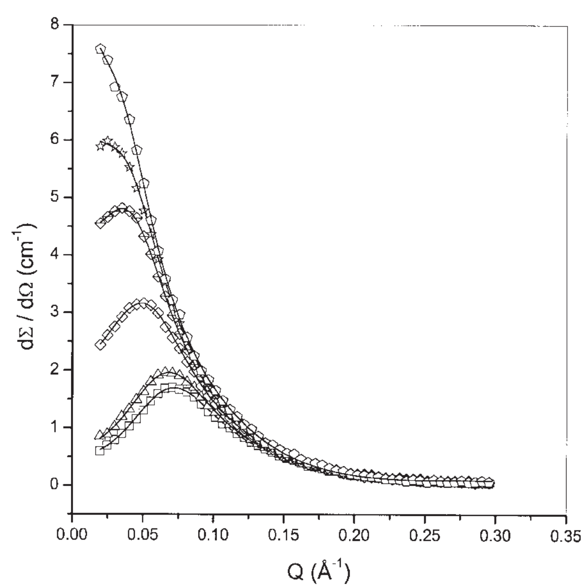

FIG. 4. SANS spectra from 100 mM SDBS solutions with increasing concentration (*x*) of Bu_4NBr at 30°C: *x* = 0.0, (open square); 5, (open triangle); 15, (open diamond); 25, (diamond with horizontal line); 32, (open star); 39.5 mM, (open pentagon). Solid lines are theoretical fits based on Hayter–Penfold-type analysis. For abbreviations see Figures 1–3.

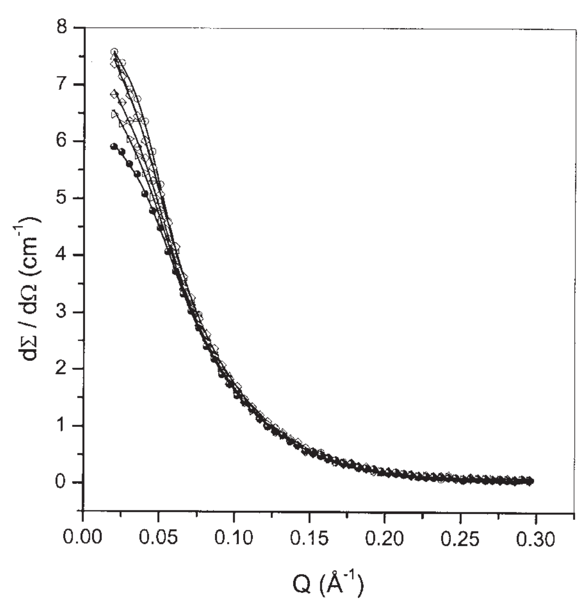

FIG. 5. SANS spectra from 100 mM SDBS + 39.5 mM Bu_4NBr system at different temperatures: 30, (open circle with centered dot); 40, (open triangle); 50, (open diamond); 60, (diamond with horizontal line); 70, (right-pointing open triangle with centered dot); 80°C, (closed circle containing off-center open dot). Solid lines are theoretical fits based on Hayter–Penfold-type analysis. For abbreviations see Figures 1–3.

TABLE 3
Micellar Parameters for 100 mM SDBS + 39.5 mM Bu_4NBr Obtained from Hayter–Penfold-Type Analysis[a] at Different Temperatures

Temperature (°C)	n_s	α	c (Å)	a = b (Å)	c/a
30	300	0.09	162.6	16.4	9.91
40	258	0.09	144.6	16.1	8.98
50	253	0.07	140.1	16.2	8.65
60	239	0.07	133.7	16.0	8.36
70	219	0.07	124.7	16.0	7.79
80	196	0.07	113.0	16.0	7.06

[a]For abbreviations see Tables 1 and 2.

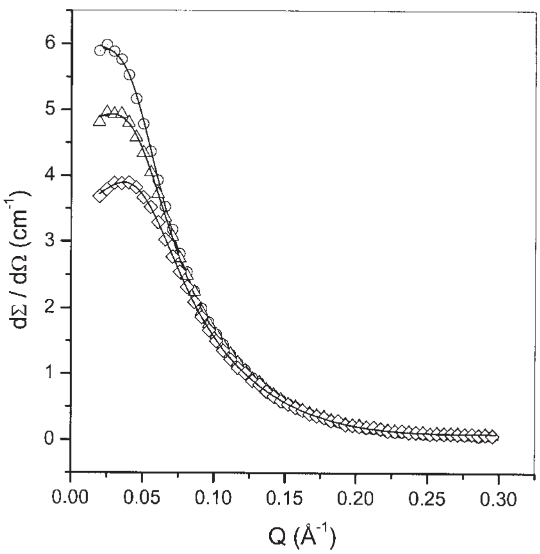

FIG. 6. SANS spectra from 100 mM SDBS + 32 mM Bu_4NBr system at different temperatures: 30, (open circle with centered dot); 60, (open triangle); 80°C, (open diamond). Solid lines are theoretical fits based on Hayter–Penfold-type analysis. For abbreviations see Figures 1–3.

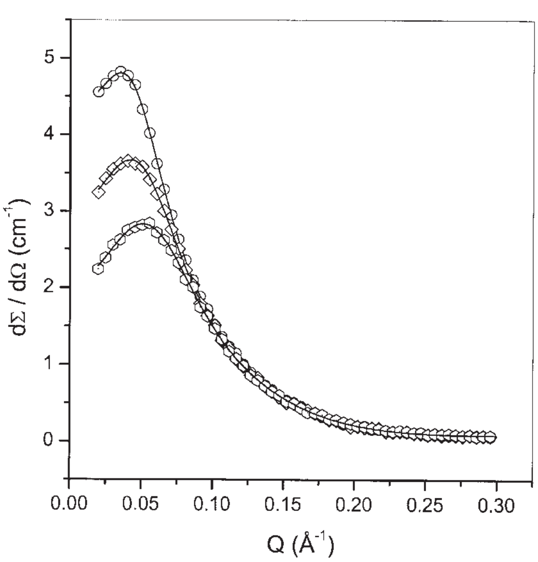

FIG. 7. SANS spectra from 100 mM SDBS + 25 mM Bu_4NBr system at different temperatures: 30, (open circle); 60, (open diamond with centered dot); 80°C, (open hexagon with centered dot). Solid lines are theoretical fits based on Hayter–Penfold-type analysis. For abbreviations see Figures 1–3.

TABLE 4
Micellar Parameters for 100 mM SDBS + 32 mM Bu_4NBr Obtained from Hayter–Penfold-Type Analysis[a] at Different Temperatures

Temperature (°C)	n_s	α	c (Å)	a = b (Å)	c/a
30	228	0.09	126.8	15.9	7.97
60	169	0.09	97.1	15.6	6.22
80	126	0.09	75.6	15.3	4.94
30[b]	298	0.06	166.7	16.91	9.86

[a]For abbreviations see Tables 1 and 2.
[b]Parameters of this row are for 50 mM SDBS + 32 mM Bu_4NBr belonging to the below-LCB (lower consolute boundary) region. For other abbreviations see Tables 1 and 2.

TABLE 5
Micellar Parameters for 100 mM SDBS + 25 mM Bu_4NBr Obtained from Hayter–Penfold-Type Analysis[a] at Different Temperatures

Temperature (°C)	n_s	α	c (Å)	a = b (Å)	c/a
30	192	0.10	109.2	15.4	7.09
60	123	0.10	73.2	15.1	4.85
80	80	0.12	52.8	14.7	3.59

[a]For abbreviations see Tables 1 and 2.

with increase in temperature. Table 4 data for 30°C show that, even with a low surfactant concentration, a significant increase in n_s has taken place. It is likely the effective salt concentration plays a major role in deciding the final aggregate morphology. The availability of limited data in this region (below LCB) does not permit any further comments. Also, the effect of temperature (Fig. 8) could not be analyzed with the existing program.

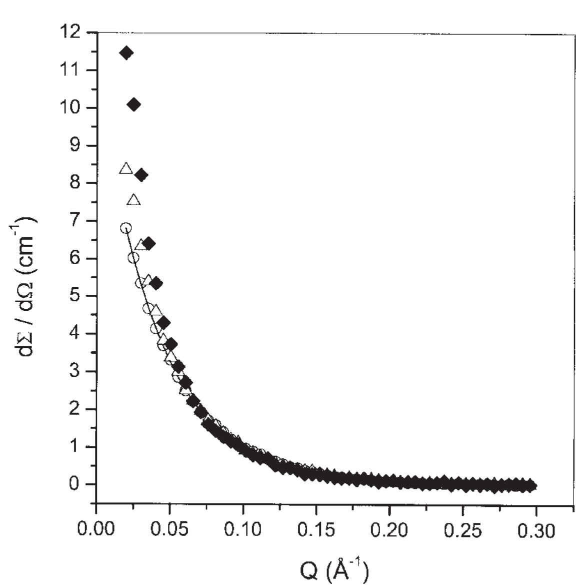

FIG. 8. SANS spectra from 50 mM SDBS + 32 mM Bu_4NBr system at different temperatures: 30, (open circle); 40, (open triangle); 50°C, (closed diamond). Solid lines are theoretical fits based on Hayter–Penfold-type analysis. For abbreviations see Figures 1–3.

ACKNOWLEDGMENTS

The work was performed under collaborative research Scheme No. IUC/CRS-M-105 of University Grants Commission—Department of Atomic Energy Consortium for Scientific Research, India. Sanjeev Kumar thankfully acknowledges the award of Senior Research Associateship [Pool Scheme No. 13 (7719-A) 2002/Pool] by the Council of Scientific and Industrial Research, New Delhi. The authors thank Dr. Prem S. Goyal, Centre Director, UGC–DAE CSR, BARC, Mumbai, and Dr. Vinod K. Aswal, Scientific Officer, Solid State Physics Division, for kind permission for SANS experiments and for valuable suggestions.

REFERENCES

1. Degiorgio, V., Critical Exponents Near the Lower Consolute Point of nonionic micellar Solutions, in *Physics of Amphiphiles*: *Micelles, Vesicles, and Microemulsion*s, edited by V. Degiorgio and M. Corti, North-Holland, Amsterdam, 1985.
2. Laughlin, R.G., Solution and Structural Requirements of Surfactant Hydrophilic Groups, in *Advances in Liquid Crystals*, edited by G.H. Brown, Academic Press, New York, 1978, Vol. 3, p. 41.
3. Warr, G.W., T.N. Zemb, and M. Drifford, Liquid–Liquid Phase Separation in Cationic Micellar Solutions, *J. Phys. Chem. 94*:3086 (1990).
4. Khan, A., B. Jonsson, and H. Wennerstrom, Phase Equilibria in the Mixed Sodium and Calcium Di-2-ethylhexylsulfosuccinate Aqueous System. An Illustration of Repulsive and Attractive Double-Layer Forces, *J. Phys. Chem*. *89*:5180 (1985).
5. Uang, Y.-J., F.D. Blum, S.E. Friberg, and J.-F. Wang, Deuterium NMR and Low-Angle X-ray Studies of a Polymerizable Liquid Crystalline System, *Langmuir 8*:1487 (1992).
6. Kumar, S., D. Sharma, Z.A. Khan, and Kabir-ud-Din, Occurrence of Cloud Points in Sodium Dodecyl Sulfate–Tetra-*n*-butylammonium Bromide System, *Langmuir 17*:5813 (2001).
7. Kumar, S., D. Sharma, Z.A. Khan, and Kabir-ud-Din, Salt-Induced Cloud Point in Anionic Surfactant Solutions: Role of the Headgroup and Additives, *Langmuir 18*:4205 (2002).
8. Kumar, S., D. Sharma, and Kabir-ud-Din, Temperature-[Salt] Compensation for Clouding in Ionic Micellar Systems Containing Sodium Dodecyl Sulfate and Symmetrical Quaternary Bromides, *Langmuir 19*:3539 (2003).
9. Mackay, R.A., Solubilization, in *Nonionic Surfactants*, Surfactant Science Series, edited by M.J. Schick, Marcel Dekker, New York, 1987, Vol. 23, p. 297.
10. Balmbra, R.R., J.S. Clunie, J.M. Corkill, and J.F. Goodman, Effect of Temperature on the Micelle Size of a Homogenous Nonionic Detergent, *Trans. Faraday Soc*. *58*:1661 (1962).
11. Macay, W.N., Factors Affecting the Solubility of Nonionic Emulsifiers, *J. Colloid Sci*. *11*: 272 (1956).
12. Vassiliaded, A.E., Coacervation in Cationic Surfactant Solutions, in *Cationic Surfactants,* Surfactant Science Series, edited by E. Jungermann, Marcel Dekker, New York, 1972, Vol. 4, p. 387.
13. Marszall, L., Cloud Point of Mixed Ionic-Nonionic Surfactant Solutions in the Presence of Electrolytes, *Langmuir 4*:90 (1988).
14. Strunk, H., P. Lang, and G.H. Findenegg, Clustering of Micelles in Aqueous Solutions of Tetraoxyethylene-*n*-octyl Ether (C_8E_4) as Monitored by Static and Dynamic Light Scattering, *J. Phys. Chem*. *98*:11557 (1994).
15. Zulauf, M., K. Weckstrom, J.B. Hayter, V. Degiorgio, and M. Corti, Neutron Scattering Study of Micelle Structure in Isotropic Aqueous Solutions of Poly(oxyethylene) Amphiphiles, *J. Phys. Chem*. *89*:3411 (1985).
16. Richtering, W.H., W. Burchard, E. Jahns, and H. Finkelmann, Light Scattering from Aqueous Solutions of a Nonionic Surfactant ($C_{14}E_8$) in a Wide Concentration Range, *J. Phys. Chem*. *92*:6032 (1988).
17. Kumar, S., V.K. Aswal, A.Z. Naqvi, P.S. Goyal, and Kabir-ud-Din, Cloud Point Phenomenon in Ionic Micellar Solution: A SANS Study, *Langmuir 17*:2549 (2001).
18. Strey, R., and A. Pakusch, *Surfactants in Solution*, edited by K.L. Mittal and P. Bothorel, Plenum Press, New York, 1987, Vol. 4, p. 465.
19. Lang, P., and Q. Glatter, Small-Angle X-ray Scattering from Aqueous Solutions of Tetra(oxyethylene)-*n*-octyl Ether, *Langmuir 12*:1193 (1996).
20. Shigeta, K., U. Olsson, and H. Kunieda, Correlation Between Micellar Structure and Cloud Point in Long Poly(oxyethylene)$_n$ Oleyl Ether Systems, *Langmuir 17*:4717 (2001).
21. Bales, B.L., and R. Zana, Cloud Point of Aqueous Solutions of Tetrabutylammonium Dodecyl Sulfate Is a Function of the Concentration of Counterions in the Aqueous Phase, *Langmuir 20*:1579 (2004).
22. Aswal, V.K., and P.S. Goyal, Small-Angle Neutron Scattering Diffractometer at Dhruva Reactor, *Curr. Sci. 79*:947 (2000).
23. Hayter, J.B., and J. Penfold, Determination of Micelle Structure and Charge by Neutron Small-Angle Scattering, *Colloid Polym. Sci. 261*:1022 (1983).
24. Bendedouch, D., S.-H. Chen, and W.C. Koehler, Determination of Interparticle Structure Factors in Ionic Micellar Solutions by Small Angle Neutron Scattering, *J. Phys. Chem*. *87*:2621 (1983).
25. Chen, S.-H., T.-L. Lin, and J.S. Huang, The Structure and Phase Transitions of a Three *Physics of Complex and Supramolecular Fluids*, edited by S.A. Safran and N.A. Clark, Wiley, New York, 1987, p. 285.
26. Hayter, J.B., and J. Penfold, Self-consistent Structural and Dynamic Study of Concentrated Micelle Solutions, *J. Chem. Soc., Faraday Trans*. *2*, *77*:1851 (1981).
27. Chen, S.-H., and T.-L. Lin, Colloidal Solutions, in *Methods of Experimental Physics*, edited by D. L. Price and K. Skold, Academic Press, New York, 1987, Vol. 23B.
28. Tanford, C., *The Hydrophobic Effect: Formation of Micelles and Biological Membrane*s, Wiley, New York, 1980.
29. Kabir-ud-Din., S.L. David, and S. Kumar, Effect of Counterion Size on the Viscosity Behaviour of Sodium Dodecyl Sulphate Micellar Solutions, *J. Mol. Liq*. *75*:25 (1998).
30. Kumar, S., V.K. Aswal, P.S. Goyal, and Kabir-ud-Din, Micellar Growth in the Presence of Quaternary Ammonium Salts: A SANS Study, *J. Chem. Soc., Faraday Trans*. *94*:761 (1998).
31. Kumar, S., S.L. David, V.K. Aswal, P.S. Goyal, and Kabir-ud-Din, Growth of Sodium Dodecyl Sulfate Micelles in Aqueous Ammonium Salts, *Langmuir 13*:6461 (1997).
32. Hayter, J.B., and M. Zulauf, Attractive Interactions in Critical Scattering from Nonionic Micelles, *Colloid Polym. Sci*. *260*:1023 (1982).

[Received June 22, 2005; accepted October 10, 2005]

Kabir-ud-Din is Professor of Physical Chemistry at Aligarh Muslim University, Aligarh, India. He received his M.Sc. (1965) and Ph.D. (1969) degrees from the same university. He has been a postdoctoral fellow in Prague (Czech Republic), Keele (United Kingdom), and Austin (Texas), and worked as an Associate Professor in Libya. His research interests are in micellar catalysis, kinetics, electrochemistry, and the solution behavior of surfactants. He has authored over 160 research papers.

Sanjeev Kumar has several years of postdoctoral research experience. He holds memberships in various scientific societies. His research areas include micellization, microemulsions, micellar growth, micellar catalysis, and clouding phenomenon. He has authored about 50 research papers.

Daksha Sharma, M.Sc., submitted her Ph.D. thesis under the supervision of Professor Kabir-ud-Din.

Deepti Sharma, M.Sc., works as a research scholar under the supervision of Professor Kabir-ud-Din.